

UCN production by multiphonon processes in superfluid Helium under pressure

P. Schmidt-Wellenburg^{a,b}, K.H. Andersen^a, O. Zimmer^{a,b}

^a*Institut Laue Langevin, 6 rue Jules Horowitz, BP-156, 38042 Grenoble Cedex 9, France*

^b*Physik-Department E18, Technische Universität München, 85748 Garching, Germany*

Abstract

Cold neutrons are converted to ultra-cold neutrons (UCN) by the excitation of a single phonon or multiphonons in superfluid helium. The dynamic scattering function $S(q, \hbar\omega)$ of the superfluid helium strongly depends on pressure, leading to a pressure-dependent differential UCN production rate. A phenomenological expression for the multiphonon part of the scattering function $s(\lambda)$ describing UCN production has been derived from inelastic neutron scattering data. When combined with the production rate from single phonon processes this allows us to calculate the UCN production for any incident neutron flux. For calculations of the UCN production from single phonon processes we propose to use the values $S^* = 0.118(8)$ at saturated vapour pressure and $S^* = 0.066(6)$ at 20 bar. As an example we will calculate the expected UCN production rate at the cold neutron beam for fundamental physics PF1b at the Institut Laue Langevin. We conclude that UCN production in superfluid helium under pressure is not attractive.

Key words: Ultracold neutron production, Superfluid helium, Helium under pressure

PACS: 78.20.Nx, 61.12.Ex, 29.25.Dz

Introduction

Current projects to increase the density of ultra-cold neutrons (UCN) available for physics experiments employ neutron converters of superfluid helium (He-II) [1,2,3] and solid deuterium [4,5,6,7,8]. In these materials cold neutrons with energies in the order of meV may be scattered down to the neV energy range by the excitation of a single phonon or multiphonon in the converter. The inverse process is suppressed by the Boltzmann factor if the converter is kept at sufficiently low temperature. We consider UCN production in He-II, for which first publications have focused on the single phonon process, where incident 8.9 Å neutrons are scattered down to the UCN energy range [9,10]. Later two publications [11,12] have set out to calculate the expected UCN production rate from processes involving the emission of two or more excitations but reached contradicting results.

The purpose of this article is to provide on the one hand a physical-model-based extrapolation to short wavelengths of scattering data relevant for UCN production. On the

other hand we consider for the first time UCN production in He-II under pressure. This is motivated by the pressure dependence of the properties of He-II, in particular its dispersion curve and density. Application of pressure to He-II increases the velocity of sound, such that the dispersion curves of He-II and of the free neutron cross at shorter neutron wavelength. For neutron beams from a neutron guide coupled to a liquid deuterium cold source, the differential flux density $d\Phi/d\lambda$ in the range 8 – 9 Å normally increases for decreasing wavelength. Pressure also increases the density of He-II. These two facts may lead to the expectation that the single phonon UCN production rate increases with pressure. Furthermore, the multiphonon contributions might be favourably affected by application of pressure. This justifies to investigate whether pressure may provide an UCN source superior to a converter at saturated vapour pressure (SVP).

The first part of this paper presents some general expressions for the UCN production rate in He-II as given in an internal note in 1982 by Pendlebury [13] and in Ref. [11]. In the second part we consider UCN production due to multiphonon scattering both for SVP and for 20 bar, using inelastic scattering data for He-II measured at 0.5 K [14]. We give a formula approximating the contribution from multi-

Email address: schmidt-w@ill.fr (P. Schmidt-Wellenburg).

phonon processes to the UCN production rate. This might be useful to calculate, for any given spectrum of incident neutrons, the expected UCN production rate. As an example, this is done here for the cold neutron beam PF1b at the Institut Laue Langevin.

UCN production rate, general expressions

UCN production in superfluid helium is due to coherent inelastic scattering of the incident cold neutrons with energy E (and wavenumber k) down to energies E' (k'). The maximum final energy is defined by the wall potential of the converter vessel (252(2) neV for beryllium) with respect to the Fermi potential of He-II (18.5 neV at SVP): $V_c = 233(2)$ neV. The production rate is given by

$$P_{\text{UCN}}(V_c) = \int_0^\infty dE \int_0^{V_c} N \frac{d\phi}{dE} \cdot \frac{d\sigma}{dE'} (E \rightarrow E') dE', \quad (1)$$

where $d\phi/dE$ is the differential incident flux, N the helium number density, and $d\sigma/dE'$ the differential cross section for inelastic neutron scattering. The latter is given by

$$\frac{d\sigma}{dE'} = 4\pi b^2 \frac{k'}{k} S(q, \hbar\omega), \quad (2)$$

where b is the neutron scattering length of ^4He , $\hbar\omega = E - E'$, $q = k - k'$, and $S(q, \hbar\omega)$ is the dynamic scattering function evaluated for values on the dispersion curve of the free neutron. Details of calculation can be found in Ref. [11] where the general result is given in Eq. (9). We may write

$$P_{\text{UCN}}(V_c) = N \sigma V_c \frac{k_c}{3\pi} \int_0^\infty \frac{d\phi}{d\lambda} s(\lambda) \lambda d\lambda, \quad (3)$$

where $\sigma = 1.34(2)$ barn [15] is the scattering cross section of ^4He , $\hbar k_c = \sqrt{2m_n V_c}$, and

$$s(\lambda) = \hbar \int S(q, \hbar\omega) \delta(\hbar\omega - \hbar^2 k^2 / 2m_n) d\omega \quad (4)$$

defines the UCN scattering function as function of the incident neutron wavelength λ , making use of $q = k = 2\pi/\lambda$, valid for $k' \ll k$. We divide it into a single and a multiphonon part, $s(\lambda) = s_I(\lambda) + s_{\text{II}}(\lambda)$.

The single phonon contribution can be approximated by $s_I(\lambda) = S^* \delta(\lambda^* - \lambda)$, where $\lambda^* = 2\pi/q^*$ is the neutron wavelength at the intersection of the dispersion curves of the free neutron and the helium ($q^* = 0.706 \text{ \AA}^{-1}$ for SVP), and $S^* = \hbar \int_{\text{peak}} S(q^*, \hbar\omega) d\omega$ denotes the intensity due to single phonon emission. Evaluation of the single-phonon UCN production rate yields

$$P_I(V_c) = N \sigma \left(\frac{V_c}{E^*} \right)^{3/2} \frac{\lambda^*}{3} \beta S^* \frac{d\phi}{d\lambda} \Big|_{\lambda^*}, \quad (5)$$

where $E^* = \hbar^2 q^{*2} / 2m_n$, and the Jacobian factor

	SVP	0 bar
λ^* [Å]	8.92(2)	8.26(2)
E^* [meV]	1.028	1.20
N [10^{22}cm^{-3}]	2.1835	2.5317
β	1.42(1)	1.21(1)
S^*	0.118(8)	0.066(7)
relative factor	1	0.41

Table 1

Factors relevant for single phonon production rate deduced from Ref. [16,17,18]. An increase in flux of a factor ~ 2.5 , going from 8.9 Å to 8.3 Å is necessary to compensate for the loss in intensity.

$$\beta = \frac{\frac{dE_n}{dq} \Big|_{q^*}}{\frac{dE_n}{dq} \Big|_{q^*} - \frac{dE_{\text{He}}}{dq} \Big|_{q^*}}$$

accounts for the overlap of the two dispersion curves, $E_n(q)$ and $E_{\text{He}}(q)$. For a beryllium-coated converter at SVP this results in

$$P_I(V_c) = 4.97(38) \cdot 10^{-8} \frac{\text{\AA}}{\text{cm}} \frac{d\phi}{d\lambda} \Big|_{\lambda^*}. \quad (6)$$

The differential multiphonon UCN production rate in the same units is given by

$$\frac{dP_{\text{II}}(V_c)}{d\lambda} = N \sigma V_c \frac{k_c}{3\pi} \frac{d\phi}{d\lambda} \lambda s_{\text{II}}(\lambda), \quad (7)$$

which depends explicitly on the form of $s_{\text{II}}(\lambda)$ which is discussed below.

UCN production rates from scattering data

The scattering function Eq. (4) can be extracted from inelastic scattering measurements. This has been done here for data previously measured by Andersen and colleagues, on the IN6 time-of-flight spectrometer at the Institut Laue Langevin, at SVP and at $p = 20$ bar. Parts of this data have already been published earlier in [14,18,19,20,21]. For the present purpose we have treated and rebinned all of the raw data to obtain a higher resolution in q and to cover the complete accessible q -range. Existing data points from previous publications were used as reference for our analysis. A typical measurement of the dynamic scattering function $S(q, \hbar\omega)$ is shown in Figure 1.

The plane is divided into slices with width $\Delta q = 0.2 \text{ \AA}^{-1}$. Figure 2 shows $S(q, \hbar\omega)$ for two representative values of q . From each such slice we extract one value of $s_{\text{II}}(\lambda)$, with λ fixed by the condition $\hbar/\lambda = \sqrt{2m_n \hbar\omega}$. For this purpose the energy is binned with width $\Delta \hbar\omega = 0.02 \text{ meV}$. The compiled data is presented in Table 2 of the appendix. For the short wavelength region below 4.5 Å only one data point exists from Ref. [19]. An accepted model for the extrapolation to short wavelengths is given by Family [22]. It was developed from low-order diagrams of the interpar-

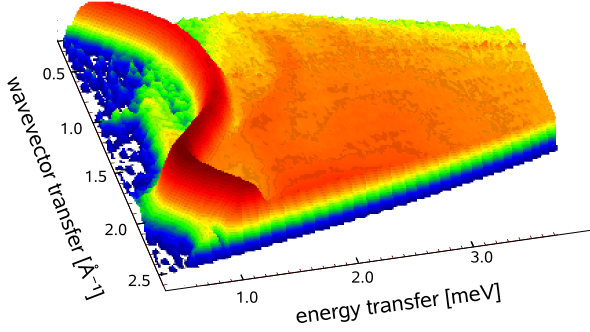


Fig. 1. Visualisation of $S(q, \hbar\omega)$, for helium at $T = 0.5$ K and $p = 20$ bar, measured by [14].

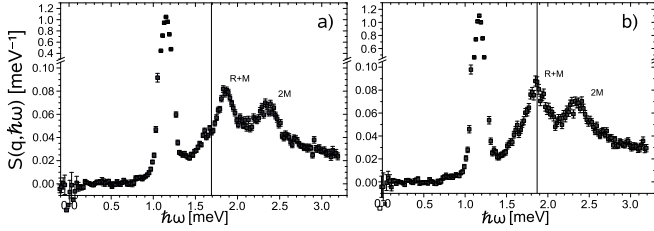


Fig. 2. $S(q, \hbar\omega)$ for a) $q = 0.90 \text{ \AA}^{-1}$ and b) $q = 0.95 \text{ \AA}^{-1}$. The vertical lines indicate the energy of an incident neutron with $E = \hbar^2 q^2 / 2m_n$ that can be down-scattered to the UCN energy range. The width of the single phonon excitation is dominated by the finite resolution of the instrument. The roton-maxon (R+M) and two maxon (2M) resonances at higher energies are significantly lower in intensity.

tile interactions in the high frequency limit and predicts $S(q, \hbar\omega) \propto q^4 \omega^{-7/2}$, which leads to $s_{II}(\lambda) \propto \lambda^3$ in our case.

For a global characterisation of the multiphonon scattering function, we have found the following analytical expression useful,

$$s_{II}(\lambda) = \frac{f\lambda^3}{\exp\left(p \cdot \frac{E_{MR} - \hbar^2/2m_n\lambda^2}{E_{rec}}\right) + 1}, \quad (8)$$

where E_{MR} is the sum of the maxon and roton energy. $E_{rec} = \frac{\hbar^2 q^2}{2m_{He}}$ is the recoil energy of the He nucleus and f, p are fitting parameters which vary with pressure (see Table 3 for values). For $\lambda < 5 \text{ \AA}$ it converges to the model of Family. In Figure 3 the correspondence of the model to the measured data is shown for SVP and 20 bar.

Both the single and the multiphonon scattering functions change with pressure. The single phonon excitation moves to shorter wavelength, β and the value for S^* decrease (see Eq. (5)). Therefore the UCN production by single phonon processes decreases as shown in Table 1, unless the cold neutron flux at 8.3 \AA is a factor of ~ 2.5 greater than at 8.9 \AA to compensate for the loss in scattering intensity. The situation looks slightly different for the UCN production rate due to multiphonon scattering. With pressure the multiphonon excitations increase in intensity and the broad peak centre moves to shorter incident-neutron wavelengths (see Figure 3). Integrating over Eq. (7) with the incident cold neutron flux of PF1b [23] at the Institut Laue Langevin, one can expect an increase in UCN produc-

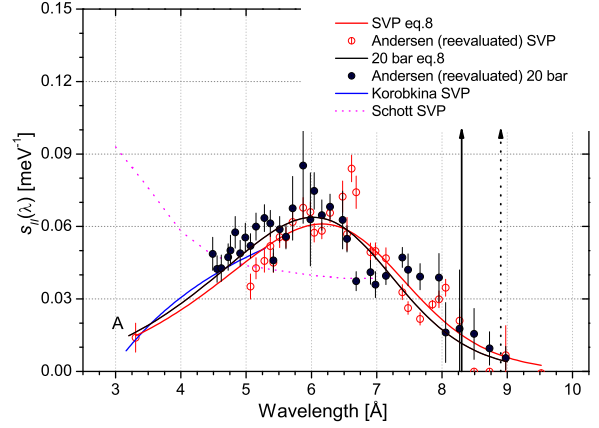


Fig. 3. Multiphonon scattering function at SVP and 20 bar. The extrapolation to short wavelength of Korobkina *et al.* [11] at SVP is linear in k , whereas the calculation of Schott *et al.* [12] is based on the static structure factor of superfluid helium. The data point (A) is taken from Ref. [19]. The one-phonon peaks are indicated by vertical arrows: SVP (\cdots) and 20 bar ($—$). The data for 20 bar include the corrections proposed in Ref. [17].

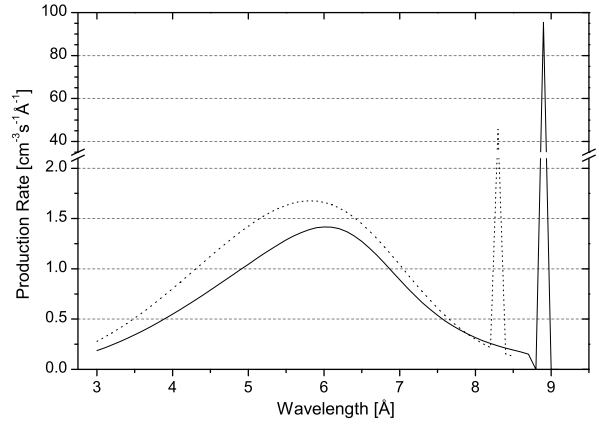


Fig. 4. Differential UCN production rate for SVP ($—$) and 20 bar ($---$) at PF1b. The calculations have been performed for a critical wall potential of 252 neV. One can see clearly the shift of the single phonon peak to shorter wavelength, as well as the subtle increase from multiphonon processes.

tion rate through multiphonon excitation. The differential production rate is shown in Figure 4. Integration over the UCN production curves for SVP and 20 bar gives in total $(13.9 \pm 0.9) \text{ cm}^{-3}\text{s}^{-1}$ and $(11.1 \pm 0.8) \text{ cm}^{-3}\text{s}^{-1}$, with a contribution of $(9.5 \pm 0.7) \text{ cm}^{-3}\text{s}^{-1}$ and $(5.8 \pm 0.4) \text{ cm}^{-3}\text{s}^{-1}$ from single phonon processes, respectively.

Discussion

We have shown how to calculate UCN production rates for different pressures based on inelastic neutron scattering

data. The single phonon UCN production rate is slightly higher than in Ref. [11] as we use for $S^* = 0.118(8)$, instead of $S^* = 0.1$. This higher value from Gibbs [18] (there called $Z(Q)$) is affirmed in a comparative analysis in Ref. [17]. A different approach by Yoshiki [24], calculating the total cross section for UCN production from single phonon excitations in a beryllium coated converter, gives a slightly larger value. However, for his numerical calculation he did not take the Fermi potential of helium into account.

A phenomenological expression is given to describe the global behaviour of the multiphonon scattering function. It converges for short incident wavelength to the model of Family. This model describes the short wavelength region better than the linear extrapolation in q used in Ref. [11], which overestimates the multiphonon contribution. The calculations done by Schott and coworkers [12] predict a huge increase in the scattering function for short wavelengths that appears to contradict the first moment sum rule [25]. Uncertainties remain in the region below 4 Å as there is only one data point available [19]. Baker and coworkers [2] have measured steadily decreasing production rates in the range of 6.5 Å to 4.5 Å. Therefore we assume to have only a small contribution to the scattering function for ≤ 4 Å, which we consider as being best represented by our expression. On the long wavelength end for $\lambda > \lambda^*$ there is no intensity, as there are no more elementary excitations in superfluid helium.

Conclusion

UCN production in superfluid helium under pressure will not lead to a gain in production rate compared to SVP using a cold neutron spectrum similar to the one of the cold beam PF1b. Only if the flux at 8.3 Å exceeds by more than 2.5 times that at 8.9 Å, an increase in UCN production rate is expected, due to the increase of intensity of multiphonon processes. However, one has to bear in mind that application of pressure requires a window for UCN extraction. Whereas, an extraction window with associated severe UCN losses can be avoided for SVP [1,3].

Appendix

References

- [1] Y. Masuda *et al.*, Phys. Rev. Lett. **89** (2002) B4801
- [2] C. Baker *et al.*, Phys. Lett. A **308** (2003) 67.
- [3] O. Zimmer *et al.*, Phys. Rev. Lett. **99** (2007) 104801
- [4] U. Trinks *et al.*, Nucl. Instr. and Meth. A **440** (2000) 666
- [5] F. Atchison *et al.*, The PSI UCN Source, ICANS-XVII, Santa Fe (2005).
- [6] A. Saunders *et al.*, Phys. Lett. B **593** (2004) 55.
- [7] A. Frei *et al.*, Eur. Phys. J. A **34** (2007) 119.
- [8] C.-Y. Liu *et al.*, APS Meeting Abstracts (1998) 210.
- [9] R. Golub, J. Pendlebury, Phys. Lett. A **82** (1977) 337.
- [10] Y. Abe, N. Morishima, Nucl. Instr. and Meth. A **463** (2001) 293.
- [11] E. Korobkina *et al.*, Phys. Lett. A **301** (2002) 462.
- [12] W. Schott *et al.*, Eur. Phys. J. A **16** (2003) 599.
- [13] internal note M. Pendlebury (1982).
- [14] M. R. Gibbs *et al.*, J. Phys.: Condens. Matter **11** (1999) 603.
- [15] V. Sears, Neutron News **3** (1992) 26.
- [16] B. M. Abraham *et al.*, Phys. Rev. A **1** (1970) 250.
- [17] F. Caupin, J. Boronat, K. H. Andersen, J. of Low Temp. Phys. **152** (2008) 108.
- [18] M. R. Gibbs, The collective excitations of superfluid ^4He : The dependence on pressure and the effect of restricted geometry, Ph.D. thesis, Keele University (1996).
- [19] B. Fåk, K. H. Andersen, Phys. Lett. A **160** (1991) 468.
- [20] W. G. Stirling, K. H. Andersen, J. of Phys. Cond. Matt. **6** (1994) A63.
- [21] M. R. Gibbs *et al.*, J. of Low Temp. Phys. **120** (2000) 55.
- [22] F. Family, Phys. Rev. Lett. **34** (22) (1975) 1374.
- [23] H. Abele *et al.*, Nucl. Instr. and Meth. A **562** (2006) 407.
- [24] H. Yoshiki, Comp. Phys. Comm. **151** (2003) 141.
- [25] A. Rahman, K. S. Singwi, A. Sjölander, Phys. Rev. **126** (3) (1962) 986.

q [\AA^{-1}]	$s(q, 20 \text{ bar})$ [meV^{-1}]	$s(q, \text{SVP})$ [meV^{-1}]
0.64		0.00428 ± 0.00288
0.66		0.1614 ± 0.00583
0.68		0.57394 ± 0.02023
0.70		0.9053 ± 0.01229
0.72	0.1000 ± 0.0069	0.75145 ± 0.011
0.74	0.2694 ± 0.0105	0.2743 ± 0.01227
0.76	0.4633 ± 0.0282	0.06861 ± 0.00488
0.78	0.3145 ± 0.0144	0.03653 ± 0.00351
0.79	0.2455 ± 0.0115	0.03015 ± 0.00347
0.80		0.02771 ± 0.00175
0.82	0.0580 ± 0.0063	0.02175 ± 0.00255
0.84	0.0420 ± 0.0076	0.02624 ± 0.00265
0.85	0.0471 ± 0.0048	0.03282 ± 0.0031
0.88	0.0395 ± 0.0042	0.04684 ± 0.00436
0.90	0.0359 ± 0.0062	0.04984 ± 0.00338
0.91	0.0410 ± 0.0057	0.04936 ± 0.00382
0.94	0.0373 ± 0.0046	0.07415 ± 0.0067
0.95		0.08398 ± 0.0055
0.96	0.0548 ± 0.0063	0.0569 ± 0.00684
0.97	0.0626 ± 0.0138	0.07238 ± 0.00648
1.00	0.0681 ± 0.0059	0.06567 ± 0.00394
1.02	0.0646 ± 0.0073	0.05824 ± 0.00336
1.04	0.0746 ± 0.0088	0.0574 ± 0.00384
1.05	0.0628 ± 0.0223	0.06596 ± 0.00425
1.07	0.0851 ± 0.0277	0.06774 ± 0.00419
1.10	0.0674 ± 0.0153	0.06188 ± 0.00442
1.12	0.0556 ± 0.0058	0.05543 ± 0.00417
1.14	0.0587 ± 0.0061	0.0556 ± 0.00431
1.16	0.0459 ± 0.0055	0.045 ± 0.004
1.17	0.0612 ± 0.0062	0.05191 ± 0.00555
1.19	0.0634 ± 0.0064	0.04576 ± 0.00472
1.22	0.0599 ± 0.0065	0.0427 ± 0.00439
1.24	0.0519 ± 0.0058	0.03515 ± 0.00518
1.26	0.0553 ± 0.0068	
1.28	0.0488 ± 0.0061	
1.30	0.0575 ± 0.0076	
1.32	0.0500 ± 0.0072	
1.33	0.0473 ± 0.0064	
1.36	0.0427 ± 0.0063	
1.38	0.0423 ± 0.0063	
1.40	0.0486 ± 0.0079	
1.90		0.014 ± 0.006

Table 2

Scattering function $s(q) = \hbar \int S(q, \hbar\omega) \delta(\hbar\omega - \hbar^2 q^2 / 2m_n) d\omega$ evaluated for UCN production at SVP and 20 bar. Blank spaces indicate that no data points are available for these wave vectors.

	SVP ($T = 1.24 \text{ K}$)	20 bar ($T = 0.5 \text{ K}$)
f [$10^{-3} \text{\AA}^{-3} \text{meV}^{-1}$]	0.3 ± 0.01	0.6 ± 0.02
p	4.46 ± 0.26	1.12 ± 0.09
E_{MR} [meV^{-1}]	1.93	1.94

Table 3

E_{MR} from Ref. [18] and fitting parameters of Eq. (8) for SVP and 20 bar, determined in a least- χ^2 fit to the inelastic scattering data.